International Journal of Current Engineering and Technology
E-ISSN 2277 – 4106, P-ISSN 2347 - 5161

Available at http://inpressco.com/category/ijcet

Research Article

Efficient Finite Element Modeling of Fiber Laser Welding Process under Conduction Regime on 316 Stainless Steel Plate

Yadaiah Nirsanametla [Á*], Swarup Bag[Á], C. P. Paul [Ḃ] and L. M. Kukreja[Ḃ]

[Á]Department of Mechanical Engineering, Indian Institute of Technology Guwahati, Guwahati 781039, Assam, India
[Ḃ]Laser Material Processing Division, Raja Ramanna Centre for Advanced Technology, Indore 452 013, India

Accepted 15 January 2014, Available online 01 February 2014, **Special Issue-2, (February 2014)**

Abstract

The research on a number of welding problems, for instance microstructural evolution, weld induced distortion and welding residual stresses, necessitates comprehensive information about the thermal history of the weldment and welded structures. In the present work, an efficient thermal model using finite element method (FEM) is developed for linear fiber laser welding process on 316 stainless steel of 3mm thick plate. In this modeling approach, the thermal conductivity of molten material is increased artificially for several folds to account the enhanced heat transfer due to high convective flow of liquid molten metal within the weld pool. In order to validate the developed FE model, a series of welding experiments are carried out using highly focused fiber laser with 800 W - 1000 W laser power and 13.33 mm/s - 18.33 mm/s laser scanning speed. The computed weld pool shapes and dimensions are compared with the experimental results at similar welding conditions. Relatively fair agreement between the numerical simulation and experimental results designates the robustness of the modeling approach followed here.

Keywords: *FEM, Thermal Analysis, Fusion Welding, Volumetric Heat Source.*

1. Introduction

Fusion welding process has been widely used to assemble several type of plates and sheets due to its many benefits over mechanical joining methods such as weight reduction, cost saving and flexibility of design. However, the fusion welding process is complex in nature due to its localized heating, melting, material flow in molten pool and solidification; very uneven thermal cycles generates in welded joint. This often causes a serious weld induced distortion and residual stresses. In order to measure weld induced distortions and residual stresses, a thorough thermal cycles necessary. In recent past the fiber laser source is becoming an important welding source over other lasers such as CO_2, Nd: YAG and diode lasers due to its advantages in terms of compact size, lower running and maintenance cost and high stability and reliability. In the present work, the authors has been studied the heat transfer analysis of fusion welding process using fiber laser as a heat source.

The most popular analytical methods for predicting the history of thermal cycles in welds was developed in the late 1940s by Rosenthal (Rosenthal, 1946 and Rosenthal, 1947) and Rykalin (Rykalin, 1974) based on fundamental theory of heat flow for moving heat source. These point and line heat source models are subject to serious errors for temperatures in and around the fusion and heat affected zones. In these models an infinity temperature at the center of heat source and insensitivity of thermal material properties were considered. Physically the welding heat sources either arc or beam should not be a point or line in nature, the heat sources will be distributed over some area with various distribution patterns. Pavelic *et al.* (Pavelic, *et al*, 1969) was introduced a Gaussian distributed 'disc' heat source model on the surface of the work piece. Even though Pavelic's 'disc' model is undoubtedly an important step forward in modeling of fusion welding heat sources, the digging action in plate thickness direction was not considered in this model. Few of the researchers (Paley, *et al*, 1975 and Westby, 1968) were considered the digging action of the welding heat source with a constant power density distribution in the fusion zone with a finite difference method but no criteria presented for assessment of the length of the weld pool. Goldak *et al.* (Goldak, *et al*, 1984) was proposed a three dimensional non-axisymmetric heat source model with 'double ellipsoid' configuration. This model is most appropriate for the welding heat source, since, the digging action of the welding heat source and the movement also incorporated for linear welding process. Wu *et al.* (Wu, *et al*, 2006) developed a new heat source model based on conical heat source model for deep penetration plasma arc welding. Moreover, the conical shape is more appropriate for the deep penetration and high aspect ratio welds.

Several investigators studied the numerical modeling of fusion welding process for measuring the weld thermal cycles and macrographs using an appropriate heat source models. De *et al.* (De, *et al*, 2003) was studied a two-

*Corresponding author:**Yadaiah Nirsanametla (yadaiah@iitg.ernet.in)**

dimensional axisymmetric finite element analysis of heat flow during laser spot welding. In this model the authors considered sensitivity of the temperature of thermal material properties and latent heat of transformations. This work was based on conduction heat transfer alone using double ellipsoidal heat source model. Frewin and Scott (Frewin, *et al*, 1999) was developed a three dimensional transient finite element model for calculation of the weld thermal cycles and weld pool dimensions during linear pulsed laser welding process (bead-on-plate welding) on AISI 1006 steel plate. Bag *et al*. (Bag, *et al*, 2009) was investigated the conduction mode laser spot welding using an adaptive heat source model with finite element method. Adaptive heat source model is not necessitating the weld pool dimensions priori to simulation. Bag *et al*. (Bag, *et al*, 2008) was developed a three dimensional quasi-steady state heat-transfer model to compute the thermal cycles and weld macrographs using an adaptive heat source model during gas tungsten arc welding process. In this model, the authors also integrated finite element model with a parent-centric recombination (PCX)–operated generalized generation gap (G3) model–based genetic algorithm to identify the magnitudes of process uncertain parameters such as process efficiency and arc radius, which are difficult to measure experimentally. The major difficulty of the double ellipsoidal heat source model is the selection of model parameters. The model parameters of Gaussian distributed double ellipsoidal heat source model can be decided with the experimental weld pool dimensions or with temperature profile of experimental investigation. Moreover, if an experimental weld pool dimensions are not available in advance; the model parameters can also be calculated using the non-dimensional model presented by Christensen *et al*. (Christensen, *et al*, 1965). Few of the researchers also studied the sensitivity of the model parameters and selection of the same. Goldak *et al*. (Goldak, *et al*, 2005) suggested that a good agreement between actual and computed weld pool size is obtained if the size selected is about 10% smaller than the actual weld pool size and the front and rear lengths are half of the width and twice the width respectively. However, the rear and front lengths may not be always true for every welding speed. Yadaiah and Bag (Yadaiah, *et al*, 2012) studied the influence of the rear and front length ratio with respect to welding speed and suggested a cubic relation between then. Few researchers (Kiran, *et al*, 2011 and Bag, *et al*, 2012) also measured the heat source model parameters with analytical method. In this approach, the shape of the weld pool volume equated with the volume of the molten material using the material properties and weld joint geometry.

In modeling of fusion welding process, the flow of molten material in weld pool plays a significant role in the assessment of the weld joint quality. Bag and De (Bag, *et al*, 2010) was investigated a transport phenomenon based heat transfer and fluid flow analysis during fusion welding process using finite element method. De and DebRoy (De, *et al*, 2006 and De, *et al*, 2005) was investigated heat transfer and fluid flow analysis during laser spot and linear welding processes respectively using finite element method along with optimization of model uncertain parameters. Yadaiah and Bag (Yadaiah, *et al*, 2013 and Bag, *et al*, 2011) was studied the influence of the surface active elements on weld pool formation during gas tungsten arc welding process. To investigate this problem, authors developed a coupled heat transfer and fluid flow model using finite element method considering the molten metal in weld pool as laminar flow. Transport phenomena based heat transfer and fluid flow models in fusion welding process are more realistic than conduction heat transfer based heat transfer analysis. However, conduction heat transfer based heat transfer analysis is often preferred due to their benefits in terms of a reduced amount of computational time, ease of modeling and its simplicity. In the present work a three dimensional transient conduction heat transfer based thermal analysis model has been developed. In this model, a Gaussian distributed double ellipsoidal volumetric heat source model implemented and the thermal conductivity is increased artificially for temperatures above the melting point in order to account the heat transfer due to molten material fluid flow in the weld pool. The experiments also performed using fiber laser to validate the computed weld pool dimensions using developed finite element model. The remaining sections of the manuscript organized as; section 2 provides a detailed experimental investigation along with process parameters and experimental setup conditions. The theoretical background of the modeling such as governing equations along with boundary conditions etc., are demonstrated in section 3. Section 4 provides a detailed results and discussions of the present study and follows the important conclusions of the present study in section 5.

2. Experimental Investigation

In order to verify the computed results accurateness of the established FE model, simple experiments were carried out to measure the weld pool dimensions and shapes. Bead-on-plate autogeneous welds were produced using a 2.0 kW ytterbium continuous-wave fiber laser on 316 stainless steel. Thickness of the specimen is 3 mm. A mixed mode laser beam power which is the mixture of two fundamental modes, 40% of TEM00 and 60% of TEM01, which gives a near flat top beam profile (Kumar, *et al*, 2008 and Kumar, *et al*, 2012) was considered.

Table 1 Experimental welding process parameters.

Data set	Laser power (W)	Welding speed (mm/s)	Heat input per unit length (J/mm)
1	1000	18.33	54.55
2	1000	13.33	75.00
3	900	18.33	49.09
4	900	13.33	67.50
5	800	18.33	43.64
6	800	13.33	60.00

The welding system consists of three major subsystems, namely, 2 kW ytterbium fiber laser, computerized numerically controlled (CNC) workstation, and CNC controller. The laser head is mounted in Z-direction vertically and movable whereas workstation is CNC

controlled and kept stationary during welding. Table 1 represents the process parameters of the welding along with net heat input per unit length.

Prior to the welding operation the work pieces were cleaned with acetone. The welded samples were kept normal to heat source. The laser welding workstation also equipped with gas on/off mode and laser power on/off mode to maintain the requirements. The fiber laser setup characteristics to conduct the welding experiments are given in Table 2.

Table 2 Experimental setup conditions during welding process

Mode of Laser Power	Continuous wave
Beam mode	Multi-mode and flat on top surface
Laser spot diameter	200µ
Beam angle	90 degrees
Wavelength	1080 nm
Shielding gas	Argon
Shielding gas flow rate	10 LPM
Fiber core diameter	50µm
Focal point	0.5 mm below to the top surface

After performing welding process the metallographic analysis was done to measure the weld pool shape and dimensions for welded samples. In the course of metallographic analysis, the welded samples were sectioned perpendicular to welding direction, polished with different grades of polishing papers (200, 400, 600, 800 and diamond polish) and etched with electrolytic etchant. The etched samples were analyzed on optical microscope. The weld pool shape and the depth of penetration and bead width are calculated for every experiment.

3. Theoretical Background

The Basic principle in heat transfer modeling of fusion welding process is the principle of conservation of energy. The general heat conduction equation for linear fusion welding process in Cartesian coordinate system when the heat source moves along Y-axis can be stated as follows

$$k\left(\frac{\partial^2 T}{\partial x^2}+\frac{\partial^2 T}{\partial y^2}+\frac{\partial^2 T}{\partial z^2}\right)+\dot{Q}=\rho c_p\left(\frac{\partial T}{\partial t}-v\frac{\partial T}{\partial y}\right) \quad (1)$$

where (x, y, z), k, T, $\dot{Q}$, ρ, c_p, t and v refer coordinate system attached to the heat source, thermal conductivity of the material, temperature variable, rate of heat generation per unit volume, density of the material, specific heat capacity of the material, time variable, and welding velocity, respectively. Figure 1 schematically represents the transverse cross-section of the weldment along with applied boundary conditions. Due to symmetric nature of the process, the half of the weld plate was considered for simulation. There is no temperature gradient normal to the weld interface i.e. symmetric surface. The top surface of the plate subjected to a specified heat flux by the cause of laser beam and the remaining surfaces (except symmetric surface) is subjected to heat losses due to convection and radiation. The natural boundary condition can be represented as

$$k_n\frac{\partial T}{\partial n}-q_s+h(T-T_o)+\sigma\varepsilon(T^4-T_o^4)=0 \quad (2)$$

where k_n, q_s, h, σ, ε and T_o denotes thermal conductivity normal to the surface, imposed heat flux, convection heat transfer coefficient, Stefan-Boltzmann constant, emissivity and ambient temperature respectively. The equation (2) is non-linear in nature and henceforth, to avoid the non-linearity, 'a lumped heat transfer coefficient' is considered in this simulation, which includes the loss due to convection and radiation. 'A lumped heat transfer coefficient can be represented as below (Goldak, *et al*, 1984)

$$h_{eff}=2.4\times10^{-3}\times\varepsilon\times T^{1.61} \quad (3)$$

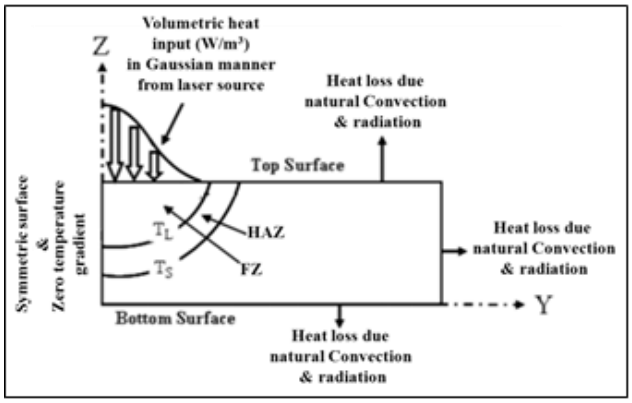

Fig.1 schematic representation the weld transverse cross-section along with applied boundary conditions

Where h_{eff} is lumped heat transfer coefficient in $W.m^{-2}.K^{-1}$, T is temperature in K and ε is the emissivity. The equation (2) can be modified by combining equations (2) and (3) as given below

$$K_n\frac{\partial T}{\partial n}-q+h_{eff}(T-T_o)=0 \quad (4)$$

The representation of the heat source in simulation was considered a Gaussian distributed double ellipsoidal volumetric heat source model (Goldak, *et al*, 1984) which is most appropriate for the conduction mode fusion welding processes. The beneficial characteristics of this kind of heat source model are the welding heat source is Gaussian distributed, the digging action included and the movement of the heat source also incorporated (front part and rear parts of the heat source are not same). If the welding heat source moves along the Y-axis, the power density distribution inside the front quadrant (f) and rear quadrant (r) for moving heat source model in Cartesian coordinate system is given by following equations

$$q_f(x,y,z)=\frac{6\times sqrt(3)\times f_f\times Q}{\pi^{3/2}\times a_f bc}\times e^{-\left[\frac{3x^2}{b^2}+\left(\frac{3y^2}{a_f^2}+\frac{3z^2}{c^2}\right)\right]} \quad (5)$$

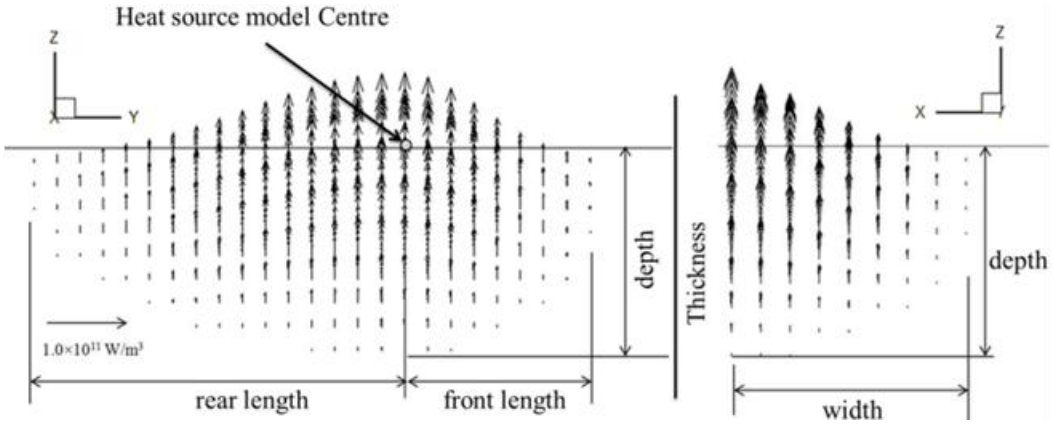

Fig.2schematic representation of the heat source model used in the present: Double ellipsoidal heat source model

$$q_r(x,y,z) = \frac{6\times\mathrm{sqrt}(3)\times f_r\times Q}{\pi^{3/2}\times a_r bc} \times e^{-\left[\frac{3x^2}{b^2}+\left(\frac{3y^2}{a_r^2}+\frac{3z^2}{c^2}\right)\right]} \quad (6)$$

where ν is welding speed, τ is a lag factor, t is time, the fractions f_f, f_r are the heat deposited parameters in the front and the rear quadrants respectively, and a_f, a_r, b, c are heat source parameters. In this work the heat source model parameters are chosen based on the experimental weld pool dimensions. There are other techniques also possible to calculate these heat source model parameters (Christensen, *et al*, 1965). Accurate results are obtained when the computed weld pool dimensions are slightly larger than the ellipsoid dimensions. In the present work, introduction section about 10% smaller than the actual weld pool dimensions. However, heat intensity Q can be expressed as

$$Q = \eta P \quad (7)$$

Where η, P are absorption coefficient and laser beam power (W) respectively; and the fraction of heat deposition parameter satisfy

$$f_f + f_r = 2 \quad (8)$$

However, the actual surface heat flux due to laser beam is replaced by double-ellipsoidal volumetric heat source. Figure 2 shows that the Gaussian distribution double ellipsoidal heat source model. From figure 2 it is obvious and has been observed that peak heat intensity is at the Centre of heat source and the distribution is Gaussian in nature over the volume of ellipsoid.

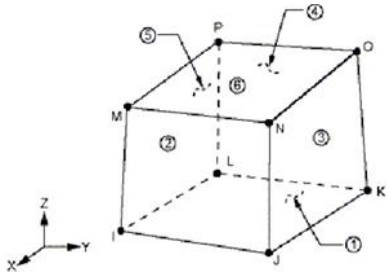

Fig.3 Schematic representation of the element SOLID 70 used (ANSYS 14.0)

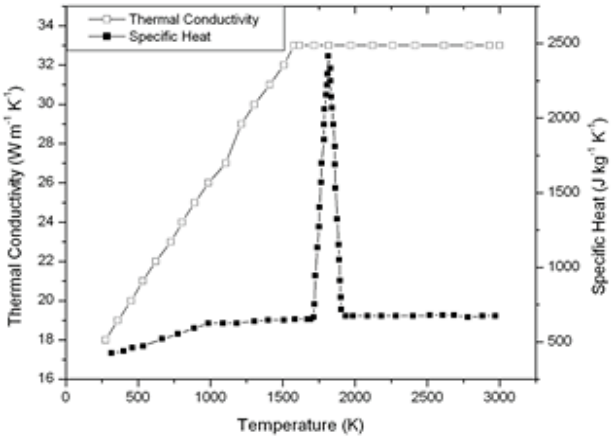

Fig.4 Temperatures dependent thermal material properties of SS316

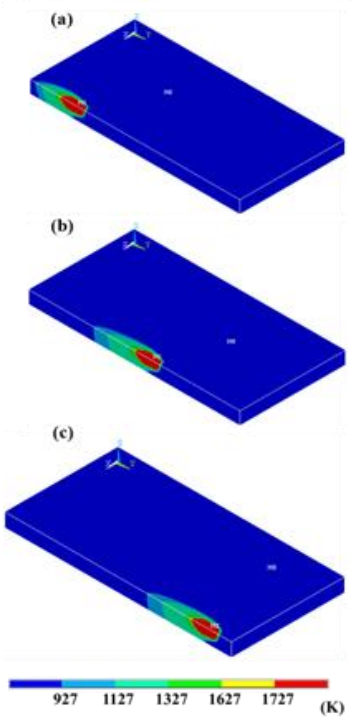

Fig.5 Three dimensional transient temperature distribution for data set 2 in table 1 at three different times; (a) at time 0.9 sec., (b) at 2.25 sec., and (c) at 3.45 sec.

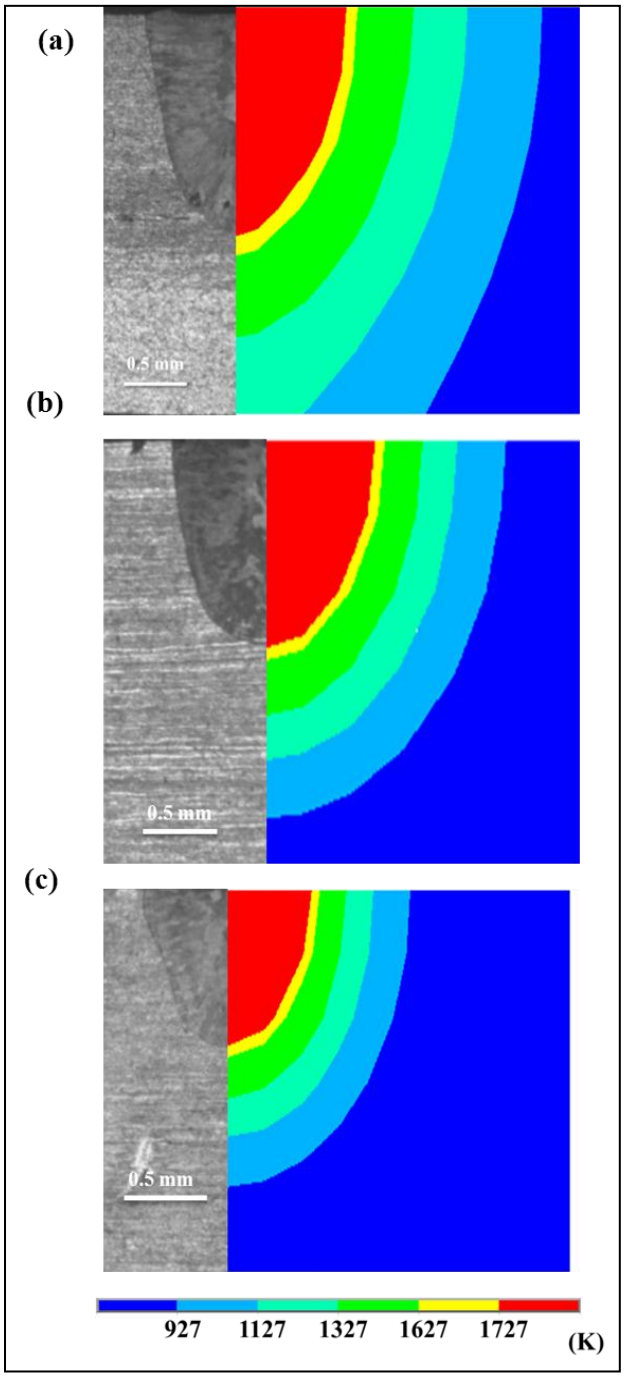

Fig.6 Comparison of experimental (left hand side) and computed (right hand side) transverse cross-section weld macrographs, (a) for data set 2 in table 1, (b) for data set 4 in table 1, and (c) for data set 6 in table 1

4. Results and Discussion

A Gaussian distributed heat source model was implemented using ANSYS APDL for determining the temperature distribution during fiber laser welding. Element SOLID 70, which is eight node brick element with temperature as degree of freedom at each node has been used and shown in figure 3 (ANSYS 14.0). The sensitivity of thermal material properties influences significantly on modeling of the welding processes (Zhu, et al, 2002).

The temperature dependent material properties (specific heat and thermal conductivity) of SS316 used in the present work and specified in figure 4 (Wang, et al, 2007 and Lindgren, et al, 1999). The density, 7200kg/m^3, the latent heat of melting and solidification was also incorporated into the material model through increase or decrease of specific heat of the material and emissivity is considered as 0.9.

Figure 5 describes the 3D transient temperature distribution for data set 2 given in table 1 at three different locations. Figure 5 (a), (b), and (c) respectively, depict the temperature distribution at time 0.9 s, 2.25 s, and 3.45 s. The region surrounded by the liquidus temperature 1727 K denotes the weld pool, and its intercepts along the Z-axis, X-axis, and Y-axis respectively represents the depth of penetration, half bead width and weld length (shown in red color). It is also observed from this figure that the temperature distribution is symmetrical about the YZ plane; on the other hand, it is asymmetric nature with respect to other planes as a result of the laser beam movement along the positive Y-axis.

Figure 6 shows the comparison between the experimentally measured (left side) and computed weld macrographs (right side). Moreover, Figures 6 (a), (b), and (c) respectively, depict the comparison of the two dimensional transverse cross-section of the experimentally observed weld pool shapes against the calculated weld macrographs for data set 2, 4, and 6 given in table 1. Furthermore, the area enclosed by the base material liquidus temperature (shown in red color), 1727 K indicates the weld molten pool and its intercepts along the, X-axis and Z-axis depict, half weld bead width and the weld penetration respectively. Figure 6 also clearly show a fair agreement between the actual weld macrographs shape and sizes and corresponding calculated weld shapes and sizes for the similar welding conditions.

Moreover, Figure 7 illustrates the measurable comparison of experimental and computed weld dimensions for welding conditions given in table 1. In figure 7, DOP and BW represent the weld depth of penetration and bead width respectively. It may be observed from the results shown in figure 7 that when keeping laser power as constant and decreasing the welding velocity, the depth of penetration increases and bead width also increases but it is nominal in magnitude. Similarly, when welding velocity is constant and decreases the laser power, weld penetration decreases and weld bead width also decreases but in this case it is substantial in magnitude.

The maximum depth of penetration is 1.64 mm for the data set 2 given in table 1 and the minimum is 0.6 mm for data set 5 given in table 1 is experimentally observed for the range of process variables given in table 1. The percentage of error between the experimentally measured weld pool dimensions and corresponding calculated weld pool dimensions are below 8 percent and this can be realized from figure 7.

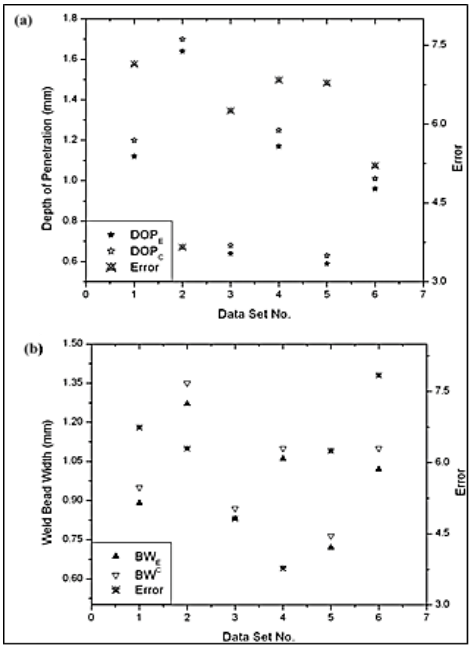

Fig.7 Quantitative comparison of calculated and experimental weld dimensions along with error between them for welding conditions given in table 1, (a) weld penetration comparisons and (b) weld bead width comparisons

5. Conclusions

In the present work, an efficient three dimensional transient heat transfer model is developed using finite element method. The fiber laser welding experiments are also conducted under conduction regime on 316 stainless steel material to validate the developed heat transfer model. The following conclusions may be drawn from this work.

1) The inclusion of temperature dependent material properties along with effective thermal conductivity of liquid material enhances the scope and utilization of conduction mode heat transfer model.
2) The volumetric heat source model with double ellipsoid configuration takes into account the digging action of high penetration laser welding process.
3) The laser power and welding velocity are most influencing process variables in fiber laser welding that actually estimates the input energy per unit length to the process. At constant laser power, the depth of penetration and bead width increase with decrease in weld velocity. However, the change of weld depth is more prominent than bead width. At constant welding velocity the decrement of weld depth and width is substantial in magnitude with decrease in laser power.
4) A fair agreement between the shape and size of actual weld macrographs and corresponding calculated values indicates the robustness of presently developed numerical model.

Acknowledgment

The authors gratefully acknowledge the financial support being provided by the Indian Institute of Technology Guwahati, Guwahati, Assam, India (grant no. SG/ME/P/SB/1) to carry out this research work. The authors thank Mr. P. Bhargava, Mr. C. H. Premsingh and Mr. S. K. Mishra for their help at various stages of experimental work.

References

D.Rosenthal,(1946), The theory of moving sources of heat and its application to metal treatments, *Transactions of ASME*, 43(11), 849-865.

D.Rosenthal,(1947), Mathematical theory of heat distribution during welding and cutting, *Welding Journal*, 20(5), 220-234.

R.R. Rykalin, Energy sources for welding, *Welding in the World* 12 (1974) 227-248.

V.Pavelic, R.Tanbakuchi, O. A.Uyehara, P. S.Myers,(1969), Experimental and computed temperature histories in gas tungsten-arc welding of thin plates, *Welding Journal*, 48(7), 295-305.

Z.Paley, P.D.Hibbert,(1975), Computation of temperatures in actual weld designs, *Welding Journal Research Supplement*, 54, 385-392.

O.Westby,(1968), Temperature distribution in the workpiece by welding, *Department of Metallurgy and Metals Working, The Technical University*, Trondheim Norway.

J.Goldak, A.Chakravarti, M.Bibby,(1984), A new finite element model for welding heat sources, *Metallurgical Transactions B*, 15B, 299-305.

C.S.Wu, H.G.Wang, Y.M.Zhang, (2006), A new heat source model for keyhole plasma arc welding in FEM analysis of the temperature profile, *Welding Journal*, 85, 284-291.

A.De, S.K.Maiti, C.Walsh, H.D.K.H.Bhadeshia,(2003), Finite element modelling of laser spot welding, *Science and Technology of Welding and Joining*, 8 (5), 377-384.

M.R.Frewin, D.A.Scott, (1999), Finite element model of pulsed laser welding, *Welding Research Supplement*, 78(1), 15-22.

S.Bag, A.Trivedi, A. De,(2009), Development of a finite element based heat transfer model for conduction mode laser spot welding process using an adaptive volumetric heat source, *Internal Journal of Thermal Science*, 48, 1923-1931.

S.Bag, A.De,(2008), Development of a three dimensional heat transfer model for GTAW process using finite element method coupled with a genetic algorithm based identification of uncertain input parameters, *Metallurgical and Materials Transactions A*, 39A (11), 2698-2710.

N.Christensen, L.de.V.Davies, Gjermundsen,(1965), Distribution of temperatures in arc welding, *British Welding Journal*, 12, 54-75.

J.A.Goldak, M.Akhlaghi,(2005), Computational welding mechanics, *Springer publication*, pp.35-36.

N.Yadaiah, S.Bag,(2012), Effect of heat source parameters in thermal and mechanical analysis of linear GTA welding process, *ISIJ International*, 52 (11), 2069-2075.

D.V.Kiran, S.Mishra, B.Basu, A.K.Shah, A.De,(2011), Three dimensional heat transfer analysis of two-wire tandem submerged arc welding, *ISIJ International*, 51 (5), 793-798.

S.Bag, D.V.Kiran, Arshad A. Syed, A.De,(2012), Efficient estimation of volumetric heat source in fusion welding process simulation, *Welding in the World*, 56(11/12), 88-97.

S.Bag, A.De,(2010), Probing reliability of transport phenomena based heat transfer and fluid flow analysis in autogeneous fusion welding process, *Metallurgical and Materials Transactions A*, 41A(9), 2337-2347.

A.De, T.DebRoy,(2006), Improving reliability of heat and fluid flow calculations during conduction model laser spot welding by multi-variable optimization, *Science and Technology of Welding and Joining*, 11(2), 143-153.

A.De, T.DebRoy,(2005), Reliable calculations of heat and fluid flow during conduction mode laser welding through optimization of uncertain parameters, *Welding Journal*, 84(7), 101-112.

N.Yadaiah, S.Bag,(2013) Role of Oxygen as Surface-Active Element in Linear GTA Welding Process, *Journal of Materials Engineering and Performance*, DOI: 10.1007/s11665-013-0621-0(online first).

S.Bag, N.Yadaiah,(2011), Possible role of surface active elements in weld pool modelling of fusion welding process, *FirstInternational Conference on Computational Methods in Manufacturing*, 154-162.

S.Kumar, S.Roy, C.P.Paul, A.K.Nath,(2008), Three-dimensional conduction heat transfer model for laser cladding process, *Numerical Heat Transfer, Part B: Fundamentals: An International Journal of Computation and Methodology*, 53 (3), 271-287.

A.Kumar, C.P.Paul, A.K.Pathak, P.Bhargava, L.M.Kukreja,(2012) A finer modeling approach for numerically predicting single track geometry in two dimensions during Laser Rapid Manufacturing, *Optics & Laser Technology*, 44 (3), 555-565.

ANSYS 14.0 Manual

X.K.Zhu, Y.J.Chao,(2002), Effect of temperature-dependent material properties on welding simulation, *Computers & Structures*, 80, 967-976.

L.Wang, S.Felicelli,(2007), Process Modeling in Laser Deposition of Multilayer SS410 Steel, *Transactions of the ASME*, 129 (1), 261-270.

L.E.Lindgren, H.Runnemalm, M.O.Nasstrom,(1999), Simulation of multipass welding of a thick plate, *International Journal for Numerical Methods in Engineering*, 44, 1301-1316.